



GENE AND CELL THERAPY

In vivo hematopoietic stem cell modification by mRNA delivery

Laura Breda^{1†}, Tyler E. Papp^{2†}, Michael P. Triebwasser^{1,3†}, Amir Yadegari², Megan T. Fedorky¹, Naoto Tanaka¹, Osheiza Abdulmalik¹, Giulia Pavani⁴, Yongping Wang^{5,6}, Stephan A. Grupp^{7,8}, Stella T. Chou^{1,5}, Houping Ni², Barbara L. Mui⁹, Ying K. Tam⁹, Drew Weissman², Stefano Rivella^{1,10,11,12,13,14*}, Hamideh Parhiz^{2*}

Hematopoietic stem cells (HSCs) are the source of all blood cells over an individual's lifetime. Diseased HSCs can be replaced with gene-engineered or healthy HSCs through HSC transplantation (HSCT). However, current protocols carry major side effects and have limited access. We developed CD117/LNP-messenger RNA (mRNA), a lipid nanoparticle (LNP) that encapsulates mRNA and is targeted to the stem cell factor receptor (CD117) on HSCs. Delivery of the anti-human CD117/LNP-based editing system yielded near-complete correction of hematopoietic sickle cells. Furthermore, in vivo delivery of pro-apoptotic PUMA (p53 up-regulated modulator of apoptosis) mRNA with CD117/LNP affected HSC function and permitted nongenotoxic conditioning for HSCT. The ability to target HSCs in vivo offers a nongenotoxic conditioning regimen for HSCT, and this platform could be the basis of in vivo genome editing to cure genetic disorders, which would abrogate the need for HSCT.

Hematopoietic stem cells (HSCs) reside in the bone marrow (BM), where they divide throughout life to produce all cells of the blood and immune system through their self-renewal ability. Their multipotency enables the formation of myeloid (erythroid, megakaryocytic, and myeloid-immune) and lymphoid cell progenitors. HSC transplantation (HSCT), which replaces diseased HSCs with healthy ones, can be a curative treatment for nonmalignant hematopoietic disorders, such as hemoglobinopathies and immunodeficiencies. Nonmalignant hematopoietic disorders can be cured with allogeneic HSCT (in which the HSC source is obtained from a sibling, parent, or unrelated donor), but only a fraction of patients have a suitable immunologic match to mini-

mize the potentially fatal complication of graft-versus-host disease (GVHD). Gene therapy can eliminate the risk of GVHD and correct nonmalignant hematopoietic disorders by using autologous HSCs (in which the HSC are obtained from the actual patient) and replace the genetic defect either through gene addition or editing. Current hematopoietic gene therapy requires isolation of HSCs from the patient and ex vivo lentiviral transduction for gene addition or electroporation with purified reagents for genome editing. A “conditioning” regimen, such as chemotherapy or radiation, is used to eliminate the patient's own HSCs. This makes space in the BM niche to allow the engraftment of infused allogeneic donor or genetically modified autologous HSCs. The conditioning procedure carries substantial acute and chronic systemic toxicities, including infertility and secondary malignancies due to accumulated DNA damage. Additionally, some nonmalignant hematopoietic disorders are due to DNA repair pathway mutations, such as radiosensitive severe combined immunodeficiency (SCID) or Fanconi anemia. These patients do not tolerate existing conditioning because of excessive toxicity with alkylating chemotherapy or radiation, as well as increased rates of malignancy long term. Therefore, we sought to address two major challenges by developing a flexible methodology that can modify HSCs in vivo and separately establish a nongenotoxic conditioning method. Here, we describe an HSC-targeted lipid nanoparticle (LNP) that encapsulates mRNA and uses antibodies against CD117 conjugated to LNP (CD117/LNP-mRNA). HSCs are dependent on stromal-derived factors, including stem cell factor (SCF), which binds to the receptor c-Kit (CD117). CD117 is expressed on both short- and long-term HSCs and some

hematopoietic progenitors (1). CD117 is internalized after the binding of SCF, which we hypothesize may facilitate or augment LNP internalization (2). Nucleoside-modified and purified mRNA is nonimmunogenic, stable, and extensible and can be used to express virtually any protein of interest (3–5). LNPs are thus far the most promising delivery system to fulfill the therapeutic potential of mRNA (6, 7). These LNPs contain ionizable lipids (positively charged at pH < 6.4), which aid in packaging the mRNA and endosomal escape. Such LNPs were first approved in 2018 for small interfering RNA (8) but became widely used in 2020 because of the LNP-mRNA platform for the Moderna and Pfizer COVID-19 vaccines. The LNP-mRNA in these US Food and Drug Administration-approved vaccines drives antigen expression but does not actively target specific cells or organs. By decorating the surface of LNPs with targeting moieties, we have demonstrated effective targeting to specific cell types, such as endothelial cells and T cells, with therapeutic efficacy upon single intravenous injection in mice, as described in our previous reports (9–11). In this work, we used nucleoside-modified mRNA that encoded cyclic AMP response element (Cre) recombinase, a CRISPR-Cas9 adenine base editor fusion gene, or the pro-apoptotic BH3-only gene PUMA (p53 up-regulated modulator of apoptosis) in CD117/LNP-mRNA to genetically alter HSCs, correct a disease mutation, or deplete HSCs through nongenotoxic conditioning, respectively. Prior studies have shown that HSC depletion through immunotoxins or radioimmunotherapy can be performed as conditioning for HSCT (12, 13), but they can only serve as platforms for HSC depletion rather than delivering other cargos. Our proof-of-principle data reveal an innovative and flexible approach to target HSCs in vivo, which may pave the way to modify HSC behavior and correct genetic mutations by delivering targeted mRNA-based therapeutics capable of genome engineering.

Results

Anti-CD117 LNPs efficiently target BM cells in vitro

We first incubated C57BL/6 lineage-depleted (Lin[−]) BM cells or whole bone marrow (WBM) in vitro with either unconjugated LNPs that encapsulated 0.1, 1, or 3 μg of nucleoside-modified luciferase mRNA (unmodified LNP-Luc), anti-CD45-conjugated LNPs (CD45/LNP-Luc), anti-CD117-conjugated LNP (CD117/LNP-Luc), or isotype control immunoglobulin G (IgG)-conjugated LNPs (control IgG/LNP-Luc). CD45/LNP and CD117/LNP were hypothesized to bind all hematopoietic-derived cells or stem and progenitor cells, respectively. Control IgG/LNP and unconjugated LNP were used as controls. The highest levels of luciferase activity in WBM were detected with CD117/LNP-Luc

¹Department of Pediatrics, Hematology, Children's Hospital of Philadelphia, Philadelphia, PA, USA. ²Division of Infectious Diseases, Perelman School of Medicine, University of Pennsylvania, Philadelphia, PA, USA. ³Department of Pediatrics, The University of Michigan, Ann Arbor, MI, USA. ⁴Department of Pathology and Laboratory Medicine, Center for Cellular and Molecular Therapeutics, Children's Hospital of Philadelphia, Philadelphia, PA, USA. ⁵Department of Pathology and Laboratory Medicine, Transfusion Medicine, Children's Hospital of Philadelphia, Philadelphia, PA, USA. ⁶Department of Clinical Pathology and Laboratory Medicine, Perelman School of Medicine at the University of Pennsylvania, Philadelphia, PA, USA. ⁷Division of Oncology, Department of Pediatrics, Children's Hospital of Philadelphia, Philadelphia, PA, USA. ⁸Departments of Pediatrics, Perelman School of Medicine, University of Pennsylvania, Philadelphia, PA, USA. ⁹Acuitas Therapeutics, Vancouver, BC V6T1Z3, Canada. ¹⁰University of Pennsylvania, Perelman School of Medicine, Philadelphia, PA, USA. ¹¹Cell and Molecular Biology affinity group, University of Pennsylvania, Philadelphia, PA, USA. ¹²Raymond G. Perelman Center for Cellular and Molecular Therapeutics, Children's Hospital of Philadelphia, Philadelphia, PA, USA. ¹³Penn Center for Musculoskeletal Disorders, Children's Hospital of Philadelphia, Philadelphia, PA, USA. ¹⁴Penn Institute for RNA Innovation, University of Pennsylvania, Philadelphia, PA, USA.

*Corresponding author. Email: rivellas@chop.edu (S.R.); hamideh.parhiz@penmedicine.upenn.edu (H.P.)

†These authors contributed equally to this work.

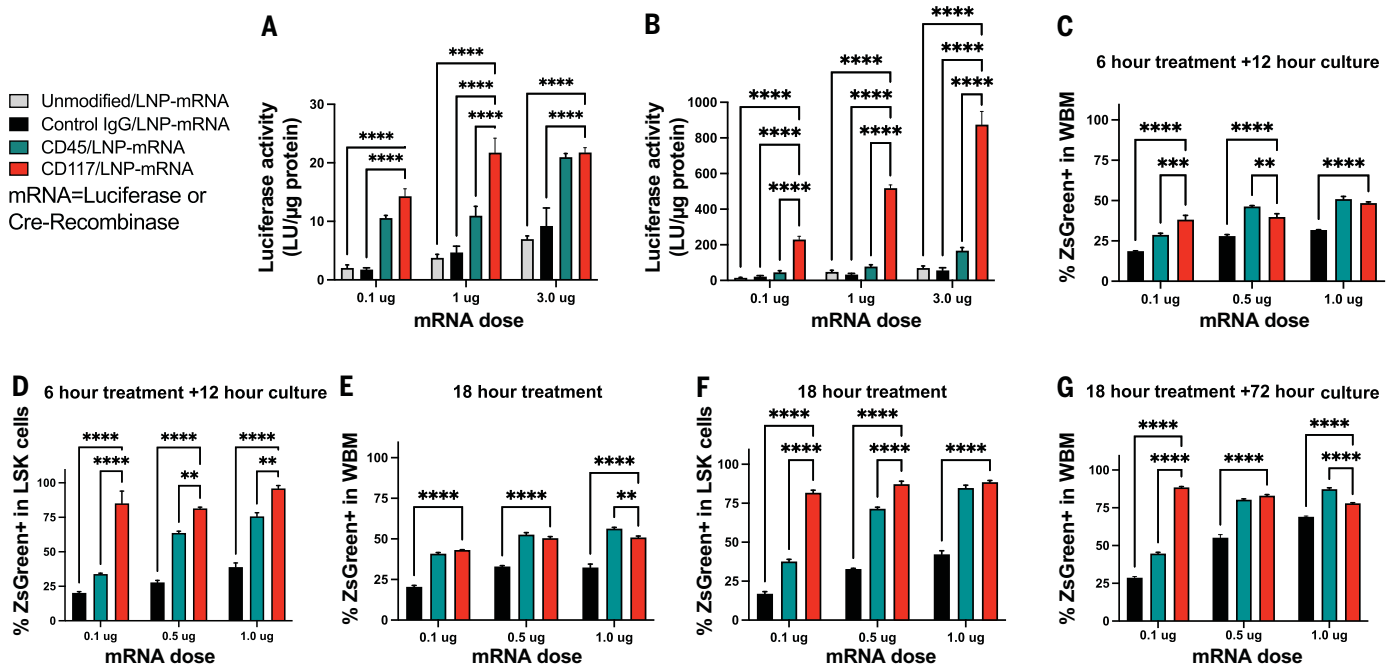


Fig. 1. In vitro targeting of WBM or hematopoietic progenitors (Lin⁻) cells incubated with LNPs that encapsulate luciferase (CD117/LNP-Luc) or Cre recombinase (CD117/LNP-Cre) mRNAs. (A) Luciferase activity normalized by total protein in WBM cells incubated with varying doses (indicated on x axis) of targeted or control LNP-Luc for 18 hours in vitro. Data indicate mean \pm SD of $n = 3$ replicate experiments. P values are from Dunnett's multiple comparison test after two-way analysis of variance (ANOVA). **** $P < 0.0001$. **(B)** LNP-Luc treatment of Lin⁻ BM ($n = 3$). Data indicate mean \pm SD of $n = 3$ replicate experiments. P values are from Dunnett's multiple comparison test after two-way

ANOVA. **** $P < 0.0001$. **(C to G)** Assessment of ZsGreen⁺ reporter induction after LNP-Cre treatments in Ai6 BM cells triggered by removal of *loxP*-flanked STOP cassette by Cre. Treatment of [(C), (E), and (G)] BM cells or [(D) and (F)] Lin⁻ BM cells at doses and culture intervals stated in figure. [(D) and (F)] LSK cell subset shown when treating Lin⁻ cells. No difference between CD117/LNP-Cre editing in Lin⁻ cells treated with 0.1 and 0.5 or 0.5 and 1 μ g. In (C) to (G), data represent mean \pm SD of $n = 3$ replicate experiments. P values are from Dunnett's multiple comparison test after two-way ANOVA. Specifically, in (C) to (G), ** $P < 0.01$, *** $P < 0.001$, **** $P < 0.0001$.

(Fig. 1A). Luciferase activity was further increased when Lin⁻ cells were treated with CD117/LNP-Luc (Fig. 1B). Increased activity of CD117/LNP-Luc in Lin⁻ cells was consistent with a 23-fold increase in the proportion of CD117⁺ in Lin⁻-selected cells (2.8% CD117⁺ in WBM cells versus 65% CD117⁺ in Lin⁻ cells). CD117/LNP luciferase activity was 500- to 700-fold greater than CD45/LNP luciferase activity in WBM depending on dose, when normalized to the frequency of CD45- and CD117-positive cells in WBM (fig. S1A). Normalized luciferase activity suggests that CD117-mediated targeting and delivery is superior to CD45-mediated targeting and functional delivery of mRNA with CD117/LNP.

CD117/LNP that encapsulated Cre recombinase mRNA (CD117/LNP-Cre) was used to test LNP-mediated genetic recombination in HSCs and persistence of the editing in conjunction with three reporter mouse models. These mouse models (Ai6, Ai9, and Ai14) are engineered with a Cre-responsive reporter allele comprised of a *loxP*-flanked STOP cassette preventing transcription of a CAG promoter-driven green or red fluorescent reporter gene (ZsGreen for Ai6 and tdTomato for Ai9 and

Ai14, respectively) inserted into the *Gt(ROSA)26Sor* locus (14). The fraction of edited WBM cells (Fig. 1C) and the subset of edited Lin⁻Scal⁺c-Kit⁺ (LSK) cells within the BM (Fig. 1D) exhibited a dose dependency (0.1 to 1 μ g mRNA) when incubated with CD45/LNP-Cre and control IgG/LNP-Cre. The majority of LNP-mediated transfections occurred within 6 hours (Fig. 1, C to F). Targeting rates in the LSK cell subset were consistently and significantly greater with CD117/LNP-Cre than with CD45/LNP-Cre or control IgG/LNP-Cre, which suggests saturation of c-Kit⁺ cells by CD117/LNP-Cre at the lowest dose tested (Fig. 1, C and D). CD117/LNP-Cre showed greater efficacy in LSK cells at lower concentrations: Treatment with 0.1 μ g CD117/LNP-Cre was 2.5-fold more effective at targeting LSK cells compared with treatment with 0.1 μ g CD45/LNP-Cre (Fig. 1D). There was no significant difference between targeted cell frequency in the LSK cell subset with the 0.1- μ g and 0.5- μ g dose or 0.5- μ g and 1- μ g dose. We also replaced the media of cells treated for 18 hours with LNP-Cre and kept them for an additional 3 days in culture to assess the maximum targeting achieved after exposing WBM to LNPs. The rate of targeted cells increased over 3 days without additional LNP

exposure (Fig. 1G): At a dose of 0.1 μ g CD117/LNP-Cre, 88.5% WBM cells were ZsGreen⁺ at 90 hours versus 43.5% at 18 hours (Fig. 1, E and G), which indicates that additional mRNA translation, Cre-mediated recombination, and ZsGreen⁺ transcription and translation occurred beyond the 18-hour LNP exposure. Notably, LNP-Cre treatment had no consistent effect on cell viability across formulations, regardless of the targeting antibody (fig. S1, B to D). Hence, we determined that the use of CD117/LNP-Cre was superior to that of CD45/LNP-Cre to modify HSCs and selected CD117-LNP-Cre for subsequent experiments.

Anti-CD117 LNPs edit multipotent and self-renewing long-term HSCs ex vivo

To evaluate multipotency in cells edited by use of CD117/LNP-Cre, we transplanted lethally irradiated congenic C57BL/6 CD45.1-recipient mice with Ai14 BM cells treated ex vivo with increasing doses of CD117/LNP-Cre and control IgG/LNP-Cre. Because HSCs give rise to all blood cell lineages, we followed reporter gene expression in peripheral blood cells over time and analyzed the BM at the 4-month endpoint (Fig. 2). The percentage of CD117/LNP-Cre-mediated tdTomato-positive Ai14 erythroid cells

in recipient mice increased with time after HSCT, which is consistent with the engraftment of donor HSC (Fig. 2C). Mice had durable editing in all lineages, specifically myeloid cells (Gr1⁺,

Fig. 2A), lymphoid cells (CD3⁺ and B220⁺, Fig. 2B), and erythroid cells (Fig. 2C) at 4 months after HSCT, which is consistent with genome editing of multipotent HSCs.

Editing rates in long-term HSCs (LT-HSC, LSK CD150⁺ CD48⁻, aka SLAM) was 95% at the 0.1- and 1- μ g mRNA dose with CD117/LNP-Cre compared with 13.5 and 20% with

Fig. 2. CD117/LNP-Cre treatment ex vivo leads to near-complete tdTomato gene editing upon transplantation.

(A and B) Percentage tdTomato marking in myeloid (Gr1⁺) (A) and lymphoid (CD3⁺, left, and B220⁺, right) (B) cells measured at 16 weeks after HSCT in lethally irradiated congenic CD45.1 recipients who received Ai14 BM treated ex vivo with 0.1 and 1 μ g of control IgG/LNP-Cre or CD117/LNP-Cre. In (A) and (B), data represent mean \pm SEM of $n = 4$ (for IgG/LNP-Cre at 1 μ g only) or $n = 5$ experimental animals per cohort. P values are from Tukey's multiple comparison test after one-way ANOVA. In (A), **** $P < 0.0001$. In (B), * $P < 0.05$, **** $P < 0.0001$.

(C) Kinetic analysis of erythroid editing measured up to 16 weeks after HSCT. Data represent mean \pm SD of $n = 4$ or 5 experimental animals per cohort. (D) tdTomato marking in the BM and BM subsets: c-Kit⁺ (Lin⁻c-Kit⁺), LSK, and LT-HSCs (SLAM). Data represent mean \pm SEM of $n = 4$ or 5 experimental animals per cohort [same animals as in (A) and (B)]. P values are Tukey's multiple comparison test after one-way ANOVA. *** $P < 0.001$, **** $P < 0.0001$. (E) CFU assay from Ai14 BM treated ex vivo with 0.1 μ g or 1 μ g of control IgG/LNP-Cre or CD117/LNP-Cre formulations or untreated.

(F and G) Semiquantitative PCR of (F) BM and (G) spleen genomic DNA isolated from the groups in (A) to (C) at 4 months after BM. **271 base pair (bp) Cre-recombinase-edited genomic DNA (gDNA) region and *1142 bp unedited region are indicated.

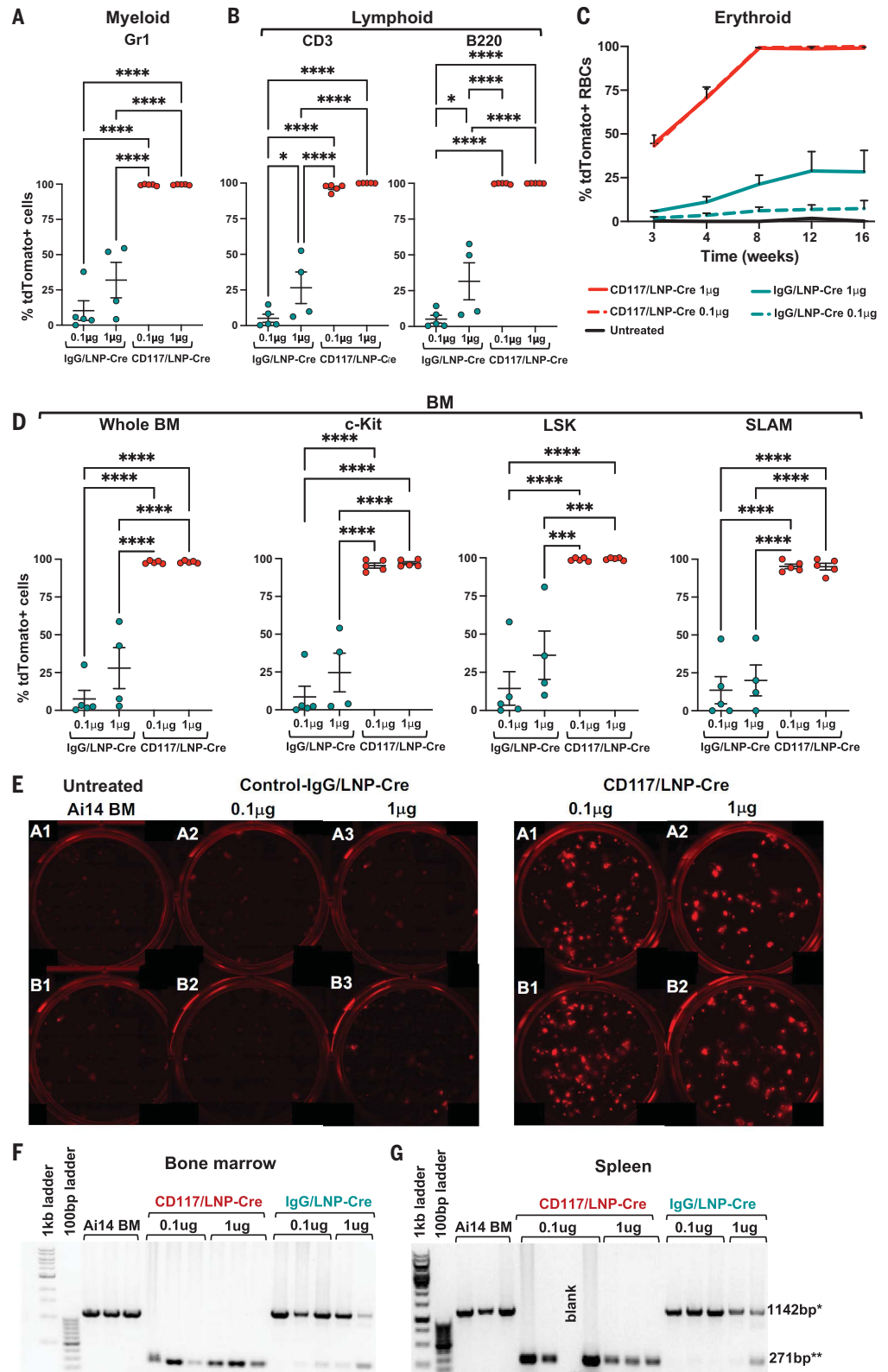


Fig. 3. CD117/LNP-Cre formulations lead to >50% tdTomato marking in LT-HSCs after in vivo injection.

(A) Biodistribution of intravenous injection of 1 μg of targeted LNP-mRNA expression in vivo by means of luminescence imaging at 24 hours. A representative sample set of dissected mouse organs were analyzed 5 min after the administration of D-luciferin.

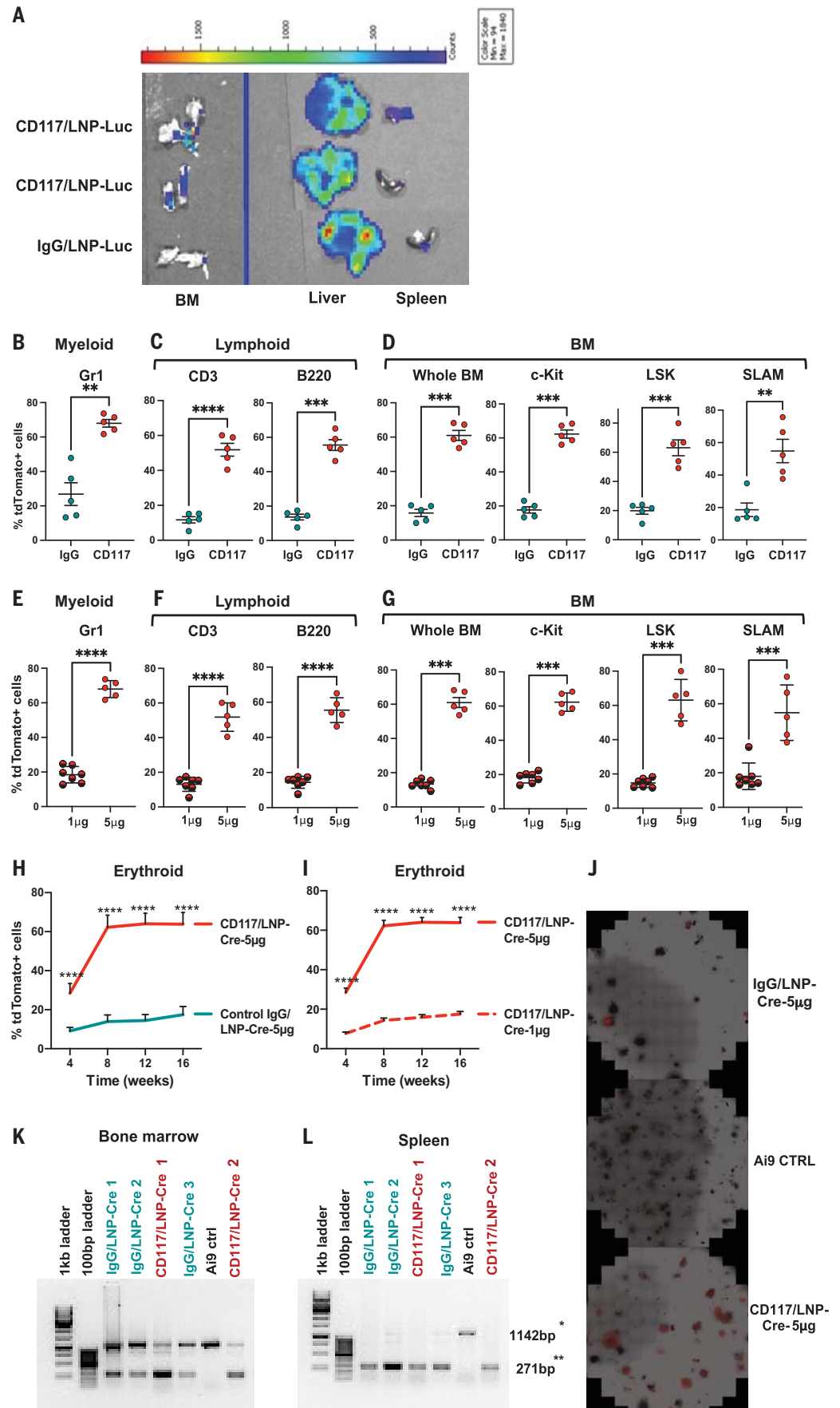
(B to D) tdTomato⁺ cell frequency in peripheral blood (B) myeloid (Gr1⁺) and (C) lymphoid cells [CD3⁺ (T cells), B220⁺ (B cells)] and in (D) BM subsets (c-Kit, LSK, SLAM/LT-HSCs) at 4 months after in vivo treatment with 5 μg of CD117/LNP-Cre or control IgG/LNP-Cre. In (B), (C), and (D), data represent mean \pm SEM of $n = 5$ experimental animals per cohort. P values are reported from paired t test. ** $P < 0.01$, *** $P < 0.001$, **** $P < 0.0001$.

(E to G) tdTomato⁺ cell frequency in peripheral blood (E) myeloid, (F) lymphoid cells, and (G) BM subsets at 4 months after in vivo treatment with 5 or 1 μg of CD117/LNP-Cre. In (E), (F), and (G), data represent mean \pm SEM of $n = 7$ (1 μg) and $n = 5$ (5 μg) experimental animals per cohort. P values are reported from t test. *** $P < 0.001$, **** $P < 0.0001$.

(H and I) Edited RBC frequency over time in *Ai9* mice treated in vivo with (H) 5 μg of CD117/LNP-Cre or control IgG/LNP-Cre or with (I) 1 or 5 μg of CD117/LNP-Cre. In (H), data represent mean \pm SD of $n = 5$ experimental animal per cohort. P values are reported from paired t test. **** $P < 0.0001$.

In (I), data represent mean \pm SD of $n = 7$ (1 μg) and 5 (5 μg) experimental animals per cohort. P values are reported from t test. **** $P < 0.0001$.

(J) CFU assay from BM at 4 months after in vivo treatment with 5 μg control IgG/LNP-Cre (top), no treatment (middle), or 5 μg CD117/LNP-Cre (bottom). **(K and L)** Semiquantitative PCR of (K) BM and (L) spleen genomic DNA isolated from the animals in (B) to (D) at 4 months after BMT. **271 bp Cre-recombinase-edited gDNA region and *1142 bp unedited region are indicated.



control IgG/LNP-Cre, respectively (Fig. 2D), which was similar to that seen in the WBM, the c-Kit⁺, and the LSK cell subsets. Donor chimerism was consistently high among all groups (>94% at 4 months) (fig. S2A). The

gene-editing rates of ex vivo-treated BM cells were dose dependent (fig. S2, B and C). Red blood cell (RBC)- and leukocyte-editing rates with CD117/LNP-Cre were ≥99% at 0.05-, 0.1-, and 1-μg mRNA doses and 91.8% at the 0.01-μg

dose (Fig. 2, A to C, and fig. S2, B to D). By comparison, targeting mediated by control IgG/LNP-Cre was near 0% at 0.01 μg (fig. S2, C and D). tdTomato⁺ Gr1⁺ cells had the fastest rise (fig. S2, B and C), which is expected given their rapid turnover of 2 to 3 days. BM cells harvested from these animals showed similar editing rates in colony-forming assays, a functional assay for clonogenic potential, and thus corroborated the flow cytometry results of LT-HSCs (Fig. 2E and fig. S2, E and F). At 4 months after HSCT, splenocytes had genome-editing levels comparable with those in the WBM (Fig. 2F, G), which is consistent with the migration of edited BM-derived cells to the spleen. To assess the stem cell potential of ex vivo-edited BM cells, we performed secondary transplants using the BM from two primary chimeras that were recipients of Ai14 BM cells treated ex vivo with either CD117/LNP-Cre or control IgG/LNP-Cre (0.1-μg dose of mRNA). Editing levels in secondary chimeras phenocopied those observed in the primary transplantation, which included sustained editing in the LT-HSC subset and editing in multiple hematopoietic lineages (fig. S3).

In vivo editing of multipotent and self-renewing long-term HSCs

Given the near-complete targeting of LT-HSCs ex vivo with CD117/LNP-Cre and our prior ability to target lung endothelial and T cells in vivo (9–11, 15), we hypothesized that LT-HSCs could be targeted in vivo as well. Intravenous administration of CD117/LNP-Luc generated luciferase activity in the femur at 24 hours, whereas IgG/LNP-Luc did not (Fig. 3A). Both control IgG/LNP-Luc and CD117/LNP-Luc showed comparable luciferase activity in the liver because LNPs bind apolipoprotein E (ApoE) and are non-specifically targeted to the low-density lipoprotein (LDL) receptor, which is expressed on hepatocytes (8). We tested in vivo multilineage editing by quantifying tdTomato expression in peripheral blood cells of intravenously IgG/ or CD117/LNP-Cre-treated animals over time (up to 4 months) and tdTomato expression in BM, and specifically the LT-HSCs, at 4 months. At the same dose (5 μg), CD117/LNP-Cre-treated mice had significantly higher editing in all peripheral blood lineages (Fig. 3, B and C) and three-fold more editing in LT-HSCs (55% versus 19%, respectively) compared with that observed in control IgG/LNP-Cre-treated mice (Fig. 3D). HSC editing after in vivo treatment with CD117/LNP-Cre was dose dependent in peripheral blood and BM at 16 weeks, with a 5.5-fold increase in the percentage of gene-edited LT-HSCs with 5 versus 1 μg (Fig. 3, E to G). LNP-Cre in vivo editing led to the appearance of edited RBCs with kinetics similar to that of the transplantation of ex vivo-treated BM (Fig. 3, H and I). At 4 months after treatment with CD117/LNP-Cre, marking of HSCs was confirmed with visual inspection of tdTomato⁺

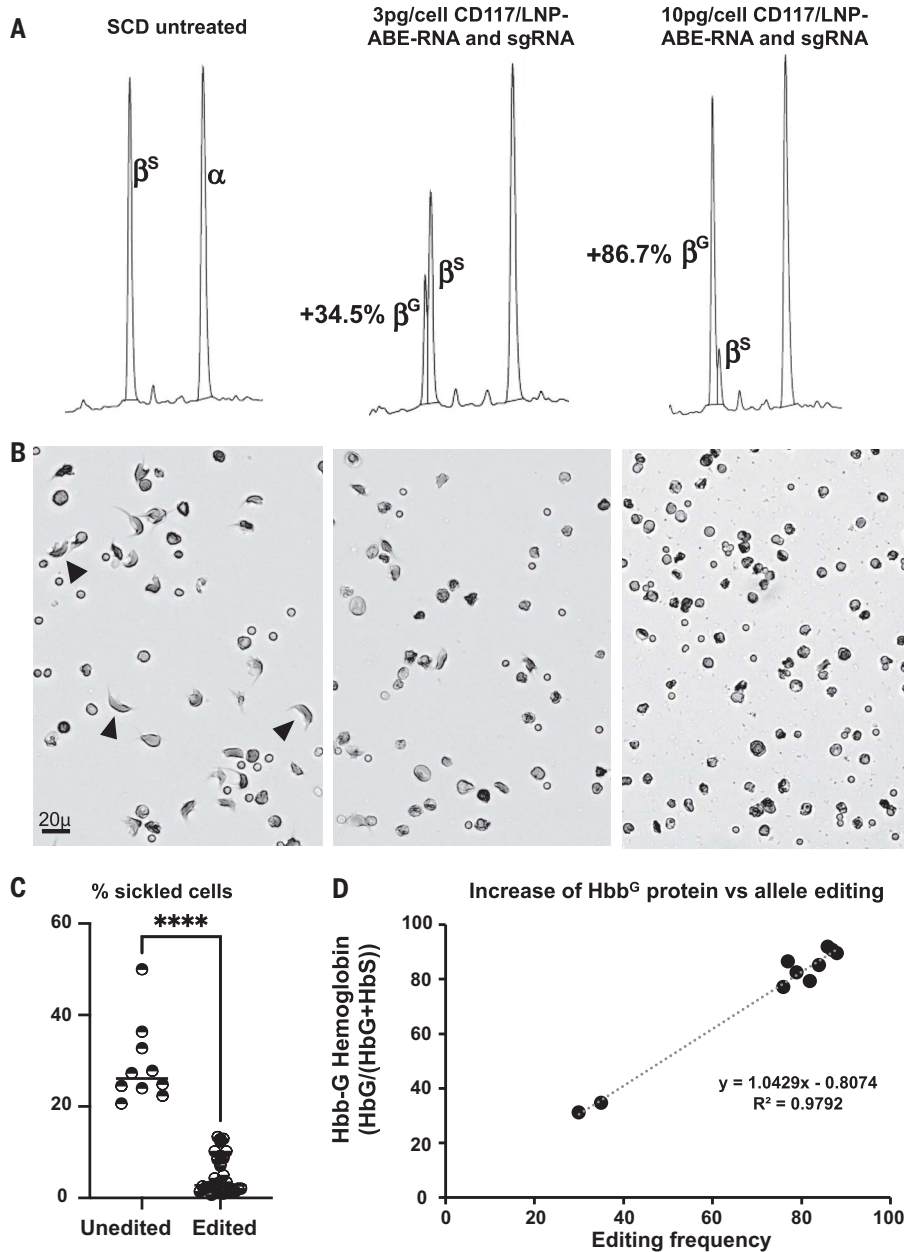


Fig. 4. Base editing of the E6V sickle cell mutation with human CD117 targeted LNP. (A) Representative reverse-phase (RP) high-performance liquid chromatography (HPLC) chromatograms of in vitro differentiated sickle cell disease (SCD) erythroid progenitor lysates untreated (left) and after treatment with anti-human CD117 (hCD117)/LNP-NRCH Cas9 ABE-8e mRNA and hCD117/LNP gRNA (middle and right). Base editing yields nonpathogenic HBB^G (β^G), which elutes before pathogenic HBB^S (β^S) and the α -globin protein (α). Percent shown is $\beta^G/(\beta^G + \beta^S) \times 100$. (B) Representative images of sickling of in vitro-differentiated erythroid progenitors under hypoxic conditions at the treatments in (A). Arrowheads indicate sickled morphology. Scale bar, 20 μm. (C) Percentage of sickled cells from unedited and edited (varying mRNA doses) sickling assays. Data represent mean \pm SD of $n = 10$ high-powered fields (hpf) (unedited specimens) and $n = 30$ hpf (edited specimens). P values are reported from unpaired t test. **** $P < 0.0001$. (D) Correlation of % β^G by RP-HPLC (protein) to base edited allele frequency (DNA).

colony-forming units (CFUs) (Fig. 3J and fig. S7A), and Cre-mediated genomic deletion in the BM and splenic DNAs was confirmed with polymerase chain reaction (PCR) (Fig. 3, K and L). To further confirm *in vivo* LT-HSC targeting, we investigated editing of the endothelial protein C receptor (EPCR)⁺ LT-HSC SLAM subpopulation (16), whose self-renewal properties are enriched compared with that of the LT-HSC SLAM population (17), using the Ai6 model (fig. S4). Editing rates in the SLAM LT-HSC population and the EPCR⁺ LT-HSC subpopulation were comparable within each cohort (CD117/LNP-Cre and Control IgG/LNP-Cre) (fig. S4E). Mice injected with CD117/LNP-Cre had 55% ± 10% edited SLAM LT-HSCs versus 46% ± 14% edited EPCR⁺ LT-HSCs, whereas mice in the control group had 9% ± 2.3% edited SLAM LT-HSCs versus 8% ± 1.9% edited EPCR⁺ SLAM LT-HSCs (fig. S4E). CFUs from the BM of primary chimeras generated from *in vivo*-

treated donors confirmed the editing differences between the two cohorts and yielded no difference in the number of colonies (fig. S4, F to H). To demonstrate that LNP-mediated editing targeted bona fide HSCs, chimeras from the initial *in vivo* experiment (Ai9 strain) were generated by transplanting irradiated congenic (C57BL/6 CD45.1) recipients with BM from mice 4 months after *in vivo* treatment with a 5-μg dose of CD117 or control IgG/LNP-Cre. Assessment of the hematopoietic-derived lineages, which included LT-HSCs in the BM, in these chimeras recapitulated editing found in the donor cells (fig. S5). LT-HSC editing in secondary chimeras was 52% for those derived from the CD117/LNP-Cre-treated primary and 19% for those derived from the control IgG/LNP-Cre-treated primary. The absolute count of viable LT-HSCs was comparable among cohorts in both primary *ex vivo* transplants and in mice injected *in vivo* (fig. S6).

Nonhematopoietic targeting after targeted LNP treatment

To quantify nonspecific cellular uptake, we compared tdTomato expression levels in lung and liver cells 4 months after *in vivo* treatment with a single dose of CD117/LNP-Cre (1- and 5-μg dose) or control IgG/LNP-Cre (5-μg dose). At 5 μg, liver editing was high (76% to 79% of cells), and editing was comparable between the two treatments (fig. S7B), which is consistent with known nonspecific ApoE and LDL receptor axis-mediated LNP uptake (8). In the lung, tdTomato expression mediated by CD117/LNP-Cre delivery was significantly higher (sevenfold) than that of mice injected with control IgG/LNP-Cre (fig. S7C). Editing observed in the perfused lung was threefold higher with 5 μg of CD117/LNP-Cre compared with 1 μg. This effect was partly “on-target” editing: Approximately 8% of lung cells were c-Kit⁺ and ~90% of lung c-Kit⁺ cells were edited (fig. S7D).

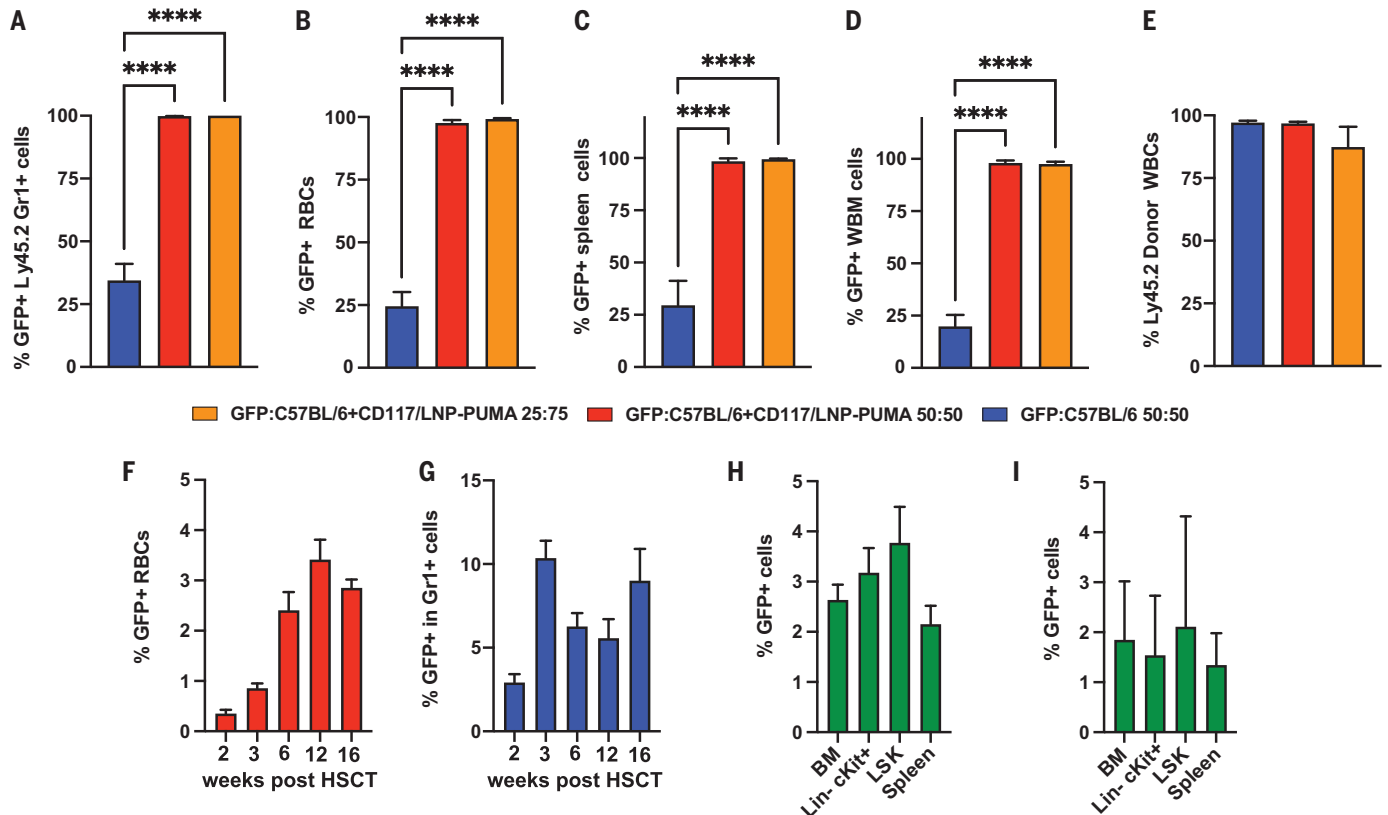


Fig. 5. HSC depletion and transplantation conditioning with CD117/LNP-PUMA. (A to D) GFP⁺ granulocytes (A) and RBCs in peripheral blood (B), as well as percentage of GFP⁺ CD45⁺ splenocytes (C) and BM cells (D) of C57BL/6 CD45.1 chimeras competitively transplanted with indicated proportion of GFP⁺ C57BL/6 BM untreated and C57BL/6 (GFP⁻) BM treated with CD117/LNP-PUMA. Data represent mean ± SD of *n* = 4 (recipients of a 25:75 ratio of GFP:C57BL/6⁺CD117/LNP-PUMA BM), *n* = 8 (recipients of a 50:50 ratio of GFP:C57BL/6⁺CD117/LNP-PUMA BM), and *n* = 4 (recipients of a 50:50 ratio of GFP:C57BL/6 untreated BM) experimental animals per cohort. *P* values calculated by means of Dunnett's multiple comparison test after one-way ANOVA. *****P* < 0.0001. (E) Donor chimerism 4 months post-HSCT. Chimerism calculated as CD45.2%/

(CD45.1%+CD45.2%). Data represent mean ± SD of the same cohorts indicated in (A) to (C). One-way ANOVA not significant (*P* > 0.05). (F) RBC, (G) granulocyte, and (H) hematopoietic cells of the BM, BM subsets, and spleen in recipients conditioned with 0.05 mg/kg CD117/LNP-PUMA and receiving 10 × 10⁶ GFP⁺ C57BL/6 BM cells at 6.5 days after treatment. Data in (F) to (H) represent mean ± SD of *n* = 3 recipient animals. Levels of GFP⁺ granulocytes and RBCs in unconditioned controls (*n* = 2) were nearly undetected (0.06 ± 0.03 and 0.05 ± 0.02, respectively) 2 months after BMT. (I) Persistence upon secondary transplantation of CD117/LNP-PUMA-conditioned GFP⁺ donor BM in lethally irradiated congenic mice. Data represent mean ± SD of *n* = 8 recipient animals generated from 3 primary chimeras.

Cells collected from the testis were also analyzed and did not show significant variations from baseline levels in control mice (fig. S7E). Additionally, none of 50 offspring sired by male mice treated with CD117/LNP-Cre in vivo ($n = 4$) or 39 offspring sired by male mice treated with control IgG/LNP-Cre ($n = 3$) in vivo expressed tdTomato. A complete list of animals evaluated is provided in table S3.

Efficient in vitro editing of primary sickle cell disease hematopoietic stem and progenitor cells with anti-human CD117

To assess the feasibility of using this platform for therapeutic human genome editing, we adapted our targeting to human CD117 and used LNPs that contained mRNA and encoded a Cas9 adenine base editor (ABE) fusion and LNPs that carried a single-guide RNA (sgRNA) targeted to the β -globin sickle cell mutation. Adenine base editing of the A to G leads to conversion of the pathogenic E6V (*HBB*^S) mutation to a nonpathogenic E6A variant (*HBB*^{G-Makassar}) (18). We applied this therapeutic strategy to convert pathogenic sickle hemoglobin (*HBB*^S) to nonpathogenic G-Makassar hemoglobin (*HBB*^G) on four sickle cell specimens from separate donors (fig. S8, A and B). We found that a molecular excess of sgRNA to ABE mRNA-containing LNPs led to efficient editing with the highest rates (88%) at 10 pg/cell dose (Fig. 4A). This led to a corresponding increase in *HBB*^G protein (up to 91.7% of β -like globin) and *HBB*^S decrease after in vitro erythroid differentiation, as well as a nearly complete absence of sickled cells upon exposure of the erythroblasts to hypoxic conditions (Fig. 4, B and C). Editing levels and the increase of *HBB*^G were directly correlated (Fig. 4D). We observed that LNP doses from 3 pg/cell up to 10 pg/cell did not alter the viability and proliferation rate of erythroid progenitor cells in vitro (fig. S8, C and D).

PUMA mRNA depletes HSCs from mouse BM in vitro

The survival of human and mouse HSCs depends on the anti-apoptotic gene *Mcl-1* (19, 20); thus, we sought to test the ability of CD117/LNP to deplete BM cells using pro-apoptotic mRNA. We tested a variety of pro-apoptotic mRNAs that act within this pathway. Among those genes tested on mouse C57BL/6 BM cells, treatment with PUMA mRNA reduced BM and LSK viability after 48 hours and 6 days in culture, respectively (fig. S9A). To confirm that LNP-PUMA mRNA treatment depleted multilineage hematopoietic stem and progenitor cell (HSPCs), we performed competitive HSCT in which C57BL/6 CD45.2 BM was treated with CD117/LNP-PUMA ex vivo (5 μ g) and transplanted at equal or increasing ratios against untreated green fluorescent protein (GFP⁺) C57BL/6 CD45.2 BM cells into lethally irradiated con-

genic C57BL/6 CD45.1 recipients (fig. S9C, schema). If CD117/LNP-PUMA efficiently depletes HSCs, mice receiving only CD117/LNP-PUMA-treated BM (C57BL/6 CD45.2) would experience BM failure from the depletion of HSCs, and those receiving competitive BM would have an overrepresentation of untreated GFP⁺ BM. The results were consistent with our expectations: Mice injected with only CD117/LNP-PUMA-treated GFP⁻ BM cells died within 2 weeks from the HSCT, which indicates that HSCs were not viable and did not engraft. Mice who received 50 or 75% CD117/LNP-PUMA-treated GFP⁻ BM had <0.5% donor GFP⁻ Gr1⁺ cells or RBCs (Fig. 5, A and B) at 4 months (endpoint) versus the expected 50 to 75%. The remainder of donor cells (CD45.2) were GFP⁺ (untreated) cells. This is consistent with the essentially complete depletion of engrafting, multilineage HSCs with ex vivo treatment of CD117/LNP-PUMA. By comparison, mice injected with control untreated GFP^{+/+} C57BL/6 CD45.2 BM at a 1:1 ratio had 25% GFP⁺ cells (Fig. 5, A to D). At endpoint, all groups had similar donor chimerism ($\geq 94\%$ C57BL/6 CD45.2) (Fig. 5E).

HSC depletion with CD117/LNP-PUMA allows for BM engraftment

HSC depletion in vivo was confirmed with intravenous injection of CD117/LNP-PUMA at 0.05 mg/kg in C57BL/6 mice, which showed a 71 and 58% decrease in the frequency of LSK cells and LT-HSCs in BM isolates 6 days after treatment, respectively (fig. S9B). A 0.05 mg/kg mRNA dose was found to be the maximum tolerated dose. Animals treated with 0.15 mg/kg or more CD117/LNP-PUMA displayed decreased activity, elevations in the alanine transaminase/aspartate transaminase (AST/ALT) ratio, venous congestion of the lungs and liver, and mortality.

We tested in vivo CD117/LNP-PUMA HSC depletion as conditioning for HSCT. After we confirmed that a liver-specific microRNA (miRNA) binding site (mir-122) could decrease expression in the liver (21) (fig. S10), we incorporated liver-specific miRNA binding sites for mir-122 into the 3' untranslated region of our PUMA mRNA cargo. mir-122 is expressed in vertebrate hepatocytes and can decrease the expression of transgenes in hepatocytes. C57BL/6 recipients received 0.05 mg/kg mRNA CD117/LNP-PUMA-miRNA intravenously 7 days before the infusion of 10×10^6 GFP⁺ C57BL/6 BM cells. The level of engraftment was evaluated after 2 weeks and up to 16 weeks (endpoint) and confirmed progressive increase and stabilization of GFP⁺ Gr1⁺ cells and RBCs, as well as hematopoietic cells in the spleen (CD45⁺) and BM (Fig. 5, F to H); 3.8% of BM LSK cells were donor. By comparison, C57BL/6-recipient mice not treated with CD117/LNP-PUMA conditioning failed to engraft donor cells. Secondary transplantation of the cells that engrafted with PUMA conditioning pheno-

typed the donors (Fig. 5I). This shows that in vivo targeting with CD117/LNP-PUMA effectively depleted HSCs, which allowed GFP⁺ BM cells to successfully engraft without need of chemotherapy or irradiation. These engraftment rates are consistent with those reported to be sufficient for the cure of SCID with healthy donor BM (22–24) and may overcome BM failure syndromes.

Concluding Remarks

Our results suggest that LNPs loaded with diverse mRNA cargos can access HSCs in the mouse BM niche in situ with a single systemic injection. Delivery efficacy to LT-HSCs in the BM niche is greatly increased by the conjugation of a targeting moiety (anti-CD117 antibody). In this work, we showed that LNPs loaded with a Cre mRNA cargo can induce durable genome editing in LT-HSCs ex vivo and in vivo at, or above, the levels reportedly required for the cure of nonmalignant hematopoietic disorders that affect the erythroid lineage with allogeneic or autologous gene-modified cells (25, 26). This approach was translated to primary human cells, for which we were able to achieve high rates of therapeutic base editing in hematopoietic cells from individuals with sickle cell disease. Additionally, we demonstrated that a genetic medicine, targeted LNP-mRNA, can leverage our understanding of HSC biology (*Mcl-1* pathway dependence) to effect cellular state change in vivo with physiologic effects. We used this system to deplete HSCs in vivo without the genotoxic conditioning regimens that often result in pulmonary, liver, and reproductive toxicity (20, 27, 28). Although this conditioning approach requires additional refinement to reduce toxicity, such as modifications to restrict LNP tropism and/or further limit gene expression in unintended cells, this has the capacity to replace current myeloablation approaches. These findings may potentially transform gene therapy in two ways. First, the cure of monogenic disorders, including nonmalignant hematopoietic disorders (hemoglobinopathies, congenital anemias or thrombocytopenias, and immunodeficiencies) and nonhematopoietic diseases (cystic fibrosis, metabolic disorders, and myopathies) with a simple intravenous infusion of targeted genetic medicines. Second, effecting cell type-specific state changes in vivo with minimal risk could allow previously impossible manipulations of physiology. Such delivery systems may help translate the promise of decades of concerted genetic and biomedical research to treat a wide array of human diseases.

REFERENCES AND NOTES

1. D. Kent et al., *Clin. Cancer Res.* **14**, 1926–1930 (2008).
2. N. S. Yee, C. W. Hsiao, H. Serve, K. Vosseller, P. Besmer, *J. Biol. Chem.* **269**, 31991–31998 (1994).
3. D. Weissman, K. Karikó, *Mol. Ther.* **23**, 1416–1417 (2015).
4. K. Karikó, M. Buckstein, H. Ni, D. Weissman, *Immunity* **23**, 165–175 (2005).

5. K. Karikó, H. Muramatsu, J. Ludwig, D. Weissman, *Nucleic Acids Res.* **39**, e142 (2011).
6. P. R. Cullis, M. J. Hope, *Mol. Ther.* **25**, 1467–1475 (2017).
7. E. Samaridou, J. Heyes, P. Lutwyche, *Adv. Drug Deliv. Rev.* **154–155**, 37–63 (2020).
8. A. Akinc *et al.*, *Mol. Ther.* **18**, 1357–1364 (2010).
9. H. Parhiz *et al.*, *J. Control. Release* **291**, 106–115 (2018).
10. O. A. Marcos-Contreras *et al.*, *Proc. Natl. Acad. Sci. U.S.A.* **117**, 3405–3414 (2020).
11. I. Tombácz *et al.*, *Mol. Ther.* **29**, 3293–3304 (2021).
12. C. T. Lutz *et al.*, *Hum. Immunol.* **28**, 27–31 (1990).
13. A. Czechowicz *et al.*, *Nat. Commun.* **10**, 617 (2019).
14. L. Madisen *et al.*, *Nat. Neurosci.* **13**, 133–140 (2010).
15. J. G. Rurik *et al.*, *Science* **375**, 91–96 (2022).
16. A. B. Balazs, A. J. Fabian, C. T. Esmon, R. C. Mulligan, *Blood* **107**, 2317–2321 (2006).
17. D. G. Kent *et al.*, *Blood* **113**, 6342–6350 (2009).
18. G. A. Newby *et al.*, *Nature* **595**, 295–302 (2021).
19. J. T. Opferman *et al.*, *Science* **307**, 1101–1104 (2005).
20. C. J. Campbell *et al.*, *Blood* **116**, 1433–1442 (2010).
21. R. Jain *et al.*, *Nucleic Acid Ther.* **28**, 285–296 (2018).
22. M. Cavazzana, E. Six, C. Lagresle-Peyrou, I. André-Schmutz, S. Hacein-Bey-Abina, *Hum. Gene Ther.* **27**, 108–116 (2016).
23. M. Cavazzana-Calvo *et al.*, *Blood* **109**, 4575–4581 (2007).
24. C. C. Dvorak *et al.*, *Biol. Blood Marrow Transplant.* **25**, 1355–1362 (2019).
25. M. Andreani *et al.*, *Haematologica* **96**, 128–133 (2011).

26. A. Miccio *et al.*, *Proc. Natl. Acad. Sci. U.S.A.* **105**, 10547–10552 (2008).
27. A. D. Leiper, *Br. J. Haematol.* **118**, 23–43 (2002).
28. A. Cohen *et al.*, *Bone Marrow Transplant.* **41** (suppl. 2), S43–S48 (2008).

ACKNOWLEDGMENTS

The authors acknowledge the Flow Cytometry Core Laboratory at the Children's Hospital of Philadelphia Research Institute for providing access to flow cytometry services. **Funding:** This research was supported by the National Institutes of Health (NIH grants 5T32HL007150 and 5T32HL007622 to M.P.T.), The Thomas B. and Jeannette E. Laws McCabe Fund at the University of Pennsylvania (to H.P.) and W. W. Smith Charitable Trust grant (to H.P.). Additional support was provided by the NHLBI U01 HL134696 (to S.T.C). **Author contributions:** Conceptualization: L.B., M.P.T., H.P., and S.R. Methodology: L.B., T.E.P., M.P.T., H.P., and S.R. Investigation: L.B., T.E.P., M.P.T., A.Y., M.T.F., N.T., H.N., B.L.M., O.A., G.P., Y.W., S.A.G., and S.T.C. Funding acquisition: H.P., S.R., and D.W. Supervision: L.B., H.P., and S.R. Writing – original draft: M.P.T., L.B., and T.E.P. Writing – review and editing: M.P.T., L.B., T.E.P., H.P., S.R., D.W., Y.K.T., and S.T.C. **Competing interests:** S.R. is a member of the scientific advisory board of Ionis Pharmaceuticals, Meira GTx, Vfior, and Disc Medicine. H.P. and D.W. are scientific founders and hold equity in Capstan Therapeutics. Y.K.T. and B.L.M. are employees and hold equity in Acuitas Therapeutics. D.W. and H.P. receive research support from BioNTech. L.B., T.E.P., M.P.T., S.R., and H.P. are inventors (University of Pennsylvania) on a patent for the in vivo gene editing of HSCs using targeted LNP for hemoglobinopathies (US Provisional Patent Application 63/499,580 filed 2 May 2023). L.B., T.E.P., M.P.T., S.R.,

and H.P. are inventors (University of Pennsylvania) on a patent for HSC-targeted LNP-mRNA for conditioning before HSC transplant (US Provisional Patent Application 63/386,754 filed 9 December 2022). D.W. and H.P. are inventors (University of Pennsylvania) on a patent on the compositions and methods for targeting LNP-mRNA therapeutics to stem cells (US Provisional Patent Application 63/182,639 filed 30 April 2021, WIPO Patent Application PCT/US2022/026933). In accordance with the University of Pennsylvania policies and procedures and our ethical obligations as researchers, D.W. and H.P. are named on additional patents that describe the use of nucleoside-modified mRNA and targeted LNPs as platforms to deliver therapeutic proteins and vaccines. These interests have been fully disclosed to the University of Pennsylvania, and approved plans are in place for managing any potential conflicts arising from licensing these patents. **Data and materials availability:** All data are available in the main text or the supplementary materials. Requests for materials should be addressed to S.R. or H.P. **License information:** Copyright © 2023 the authors, some rights reserved; exclusive licensee American Association for the Advancement of Science. No claim to original US government works. <https://www.science.org/about/science-licenses-journal-article-reuse>

SUPPLEMENTARY MATERIALS

[science.org/doi/10.1126/science.ade6967](https://doi.org/10.1126/science.ade6967)
Materials and Methods
Figs. S1 to S10
Tables S1 to S3
References (29–34)

Submitted 5 October 2022; resubmitted 18 March 2023
Accepted 1 June 2023
[10.1126/science.ade6967](https://doi.org/10.1126/science.ade6967)